

李永华. 2025. 基于短周期密集台阵接收函数成像揭示阿尔金山隆升机制. 地球与行星物理论评 (中英文), 56(1): 102-105. doi: 10.19975/j.dqyxx.2024-015.

Li Y H. 2025. Receiver function imaging based on short-period dense array reveals the uplift mechanism of the Altyn Tagh Mountains. Reviews of Geophysics and Planetary Physics, 56(1): 102-105 (in Chinese). doi:10.19975/j.dqyxx.2024-015.

基于短周期密集台阵接收函数成像揭示阿尔金山隆升机制

李永华^{1,2*}

1 中国地震局地球物理研究所, 北京 100081

2 中国地震局震源物理重点实验室, 北京 100081

doi: 10.19975/j.dqyxx.2024-015

中图分类号: P315

文献标识码: A

新生代印度—欧亚板块持续碰撞导致了青藏高原的隆升及陆内大型边界断裂的形成 (Yin and Harrison, 2000). 阿尔金断裂系是地球上规模最大的走滑断裂系统之一 (Molnar and Dayem, 2010), 长 1600 km, 由 NEE 走向的阿尔金左旋断裂和北侧的北阿尔金断裂以及两断裂之间夹持的菱形阿尔金山脉组成 (Cowgill et al., 2003).

作为青藏高原北缘主控边界, 阿尔金断裂系统在印度—欧亚板块碰撞过程中对高原地壳变形起到了重要的调节作用. 一种观点认为阿尔金断裂表现为左旋走滑运动, 而北阿尔金断裂表现为逆冲性质为主, 左旋走滑量有限, 小于 30 km (Yue and Liou, 1999; Yue et al., 2004). 另一种观点认为, 阿尔金断裂与北阿尔金断裂均为左旋走滑断裂, 且北阿尔金断裂的左旋位移量超过 120 km (Cowgill et al., 2000, 2003; Yin et al., 2002). 近年更有研究认为北阿尔金断裂在中新世中期由左旋走滑转变为逆冲断裂 (Gao et al., 2022).

对阿尔金断裂系深部结构时空演化的研究, 将有助于深入理解大陆岩石圈如何响应远场的陆陆碰撞作用. 已有深部地球物理观测表明塔里木地壳正在向阿尔金山下方底冲 (underthrusting), 然而对底冲深度的认识仍存在分歧 (Gao et al., 2001; 史大年等, 2007; Wittlinger et al., 1998; Zhang et al., 2015; Zhao et al., 2006). 远震体波层析成像 (Wittlinger et al., 1998) 和大地电磁测深研究 (Zhang et al.,

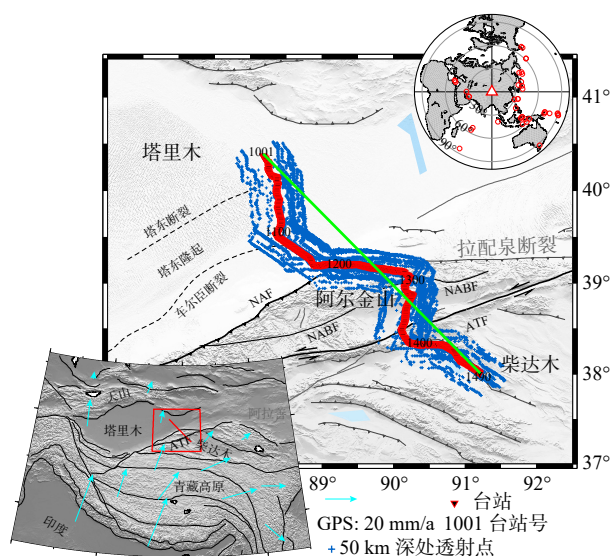


图 1 阿尔金山构造背景及密集台阵剖面 (引自 Wu et al., 2024). 红色三角形为台站位置; 蓝色十字为 Ps 转换波 50 km 深度穿透点, 绿线为 CCP 成像剖面. 右上角小图为所使用远震事件. 左下角小图为青藏高原及周边构造单元图, 红框和红线分别代表研究区和测线, 蓝色箭头为平均 GPS 速度场. NAF: 北阿尔金断裂; NABF: 北阿尔金分支断裂; ATF: 阿尔金断裂

Fig. 1 Tectonic setting the Altyn Tagh Range and the location the dense seismic array (from Wu et al., 2024). The red triangles indicate the stations of the dense array. The blue crosses show the piercing points at 50 km depth for Ps conversions. The green line shows the imaging profile. The upper-right inset shows the employed earthquake events. The lower-left inset is the map of the Qinghai-Xizang Plateau and surrounding tectonic units. The red box and the red line present the study region and the dense array, respectively. The light-blue arrows denote the average GPS velocity field. NAF, North Altyn Faults; NABF, North Altyn Branch Fault; ATF, Altyn Tagh Fault

收稿日期: 2023-04-13; 录用日期: 2024-04-15

基金项目: 第二次青藏高原综合科学考察研究项目资助 (2019QZKK0701-02)

Supported by the Second Qinghai-Xizang Plateau Scientific Expedition and Research Program (Grant No. 2019QZKK0701-02)

*通信作者: 李永华 (1975-), 男, 研究员, 主要研究方向为地震学. E-mail: liyh@cea-igp.ac.cn



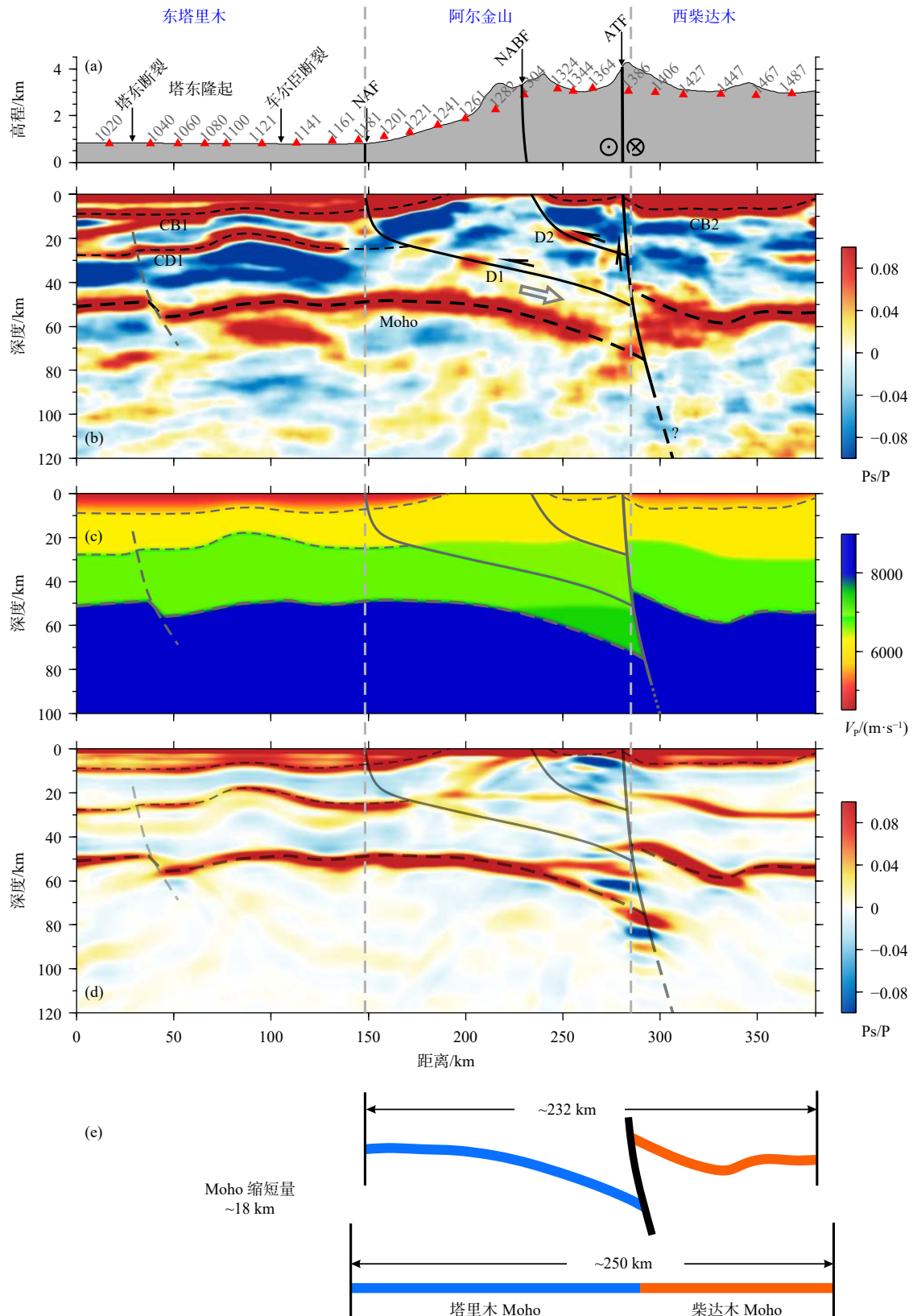


图 2 实际 CCP 图像与合成记录 CCP 图像对比 (引自 Wu et al., 2024)。(a) 地形及台站；(b) 实际 CCP 图像；(c) 基于图 (b) 构建的二维 V_p 速度模型；(d) 基于图 (c) 进行波场模拟得到的合成地震记录 CCP 成像结果；(e) 平衡剖面分析得到的跨阿尔金山新生代地壳缩短量

Fig. 2 Comparison of the observed and synthetic CCP images (from Wu et al., 2024). (a) The station locations and surface topography along the profile. (b) Observed CCP image of the crustal structure. (c) Two-dimensional V_p velocity constructed based on panel (b). (d) Synthetic CCP image for the preferred velocity model (c). (e) Estimation of the Cenozoic crustal shortening across the ATR based on the balanced cross-section of Moho length

2015) 显示塔里木地壳以陡角度向南底冲到阿尔金山断裂下方约 100 km 深处, 然而接收函数成像显示塔里木地壳则以低角度底冲至约 70 km 深处 (史大年等, 2007). 另外, 阿尔金山断裂究竟为超壳断裂, 还是壳内断裂也存在争议 (Zhao et al., 2006).

针对以上争议, Wu 等 (2024) 通过开展跨塔里木—阿尔金—柴达木的短周期密集地震剖面观测 (图 1), 利用接收函数 CCP 成像揭示了研究区清晰的 Moho 及壳内结构, 同时利用波场模拟得到了合成记录 CCP 图像, 与密集台阵 CCP 图像基本特征一致, 证明了地壳结构的可靠性 (图 2), 很好地揭示了塔里木块体向阿尔金山下方的底冲作用 (underthrusting). 作者利用平衡剖面方法, 得到阿尔金山断裂系统 NW-SE 方向缩短~18 km, 并基于地壳缩短速率 (Molnar et al., 1987; Wang et al., 2020), 推测显著的区域地壳缩短始于 9—5 Ma, 说明阿尔金山抬升主要始于晚中新世. Wu 等 (2024) 结果还显示该测线下方 Moho 深度变化剧烈, 东塔里木为 50 km, 向东南至阿尔金山下方渐变为 75 km, 至西柴达木突变为 45~54 km. 阿尔金山断裂两侧约 30 km 的 Moho 错断表明其为超壳断裂. 文章观测到东塔里木地壳为异常高 V_p/V_s , 表明有大量镁铁质物质加入, 为二叠纪地幔柱与岩石圈相互作用 (Xu et al., 2021) 提供了地震学证据. 对于阿尔金山下地壳楔状形态, 文章提出是塔里木底冲楔成因 (图 3), 同时认为底冲楔发生了部分榴辉岩化, 可能是导致其高速 (Zhao et al., 2006)、高密度 (Deng et al., 2017) 和高布格重力异常的主要因素. 综合 CCP 图像及多种观测结果, 文章提出了阿尔金山的隆升机制: 晚中新世以来, 塔里木下地壳向阿尔金山下方底冲, 塔里木和柴达木块体的斜向汇聚导致上地壳物质沿北阿尔金山逆冲断裂挤出, 形成冲起构造 (pop-up structure), 造就了阿尔金山 (图 3).

Wu 等 (2024) 揭示的塔里木下地壳底冲至阿尔金山下方的地震学图像, 为青藏高原北边界的形成演化、高原的隆升及扩展模式提供了关键的深部证据, 同时为短周期密集台阵研究典型构造域的深部结构及动力学过程提供了范式. 然而, 仍然有一些问题有待厘清. 例如, 本文中断层的深部几何形态依赖于较弱正振幅的推测, 故断裂带在下地壳乃至上地幔的几何结构仍然存在一定的不确定性. 再如, 文章成像结果较为清晰地揭示了阿尔金山断裂系的精细结构, 但未能刻画阿尔金山断裂南侧逆冲断裂

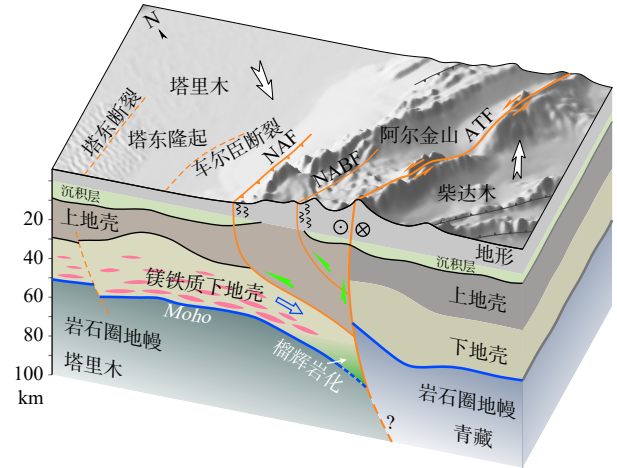


图 3 塔里木下地壳向青藏高原下方底冲 (underthrusting) 模型图 (引自 Wu et al., 2024). 白色箭头表示 GPS 观测指示的块体相对运动方向. 铁镁质塔里木下地壳底冲 (蓝色箭头) 至阿尔金山下方约 75 km 处, 底冲楔经历了部分榴辉岩化. 斜向汇聚力导致上地壳物质沿着北阿尔金山断裂及其分支断裂挤出 (绿色箭头), 形成阿尔金山的冲起构造

Fig. 3 Cartoon for the Tarim lower crust underthrusting beneath the Qinghai-Xizang Plateau (from Wu et al., 2024). The white arrows represent the relative movement indicated by GPS observations. The mafic Tarim lower crust is underthrusting to approximately 75 km beneath the Xizang, and the underthrusting wedge experienced partial eclogitization. Oblique convergence forced the upper crustal materials to be extruded along the two faults NAF and NABF, resulting in the pop-up structure of Alayn Tagh Range

系的深部特征, 建议未来地震测线向南扩展, 覆盖南部逆冲断裂系, 以查明该断裂系与阿尔金山断裂系之间的构造关系, 进而全面地认识青藏高原北缘的隆升及扩展模式. 另外, 关于中新世中期北阿尔金山断裂变形方式转变的机制仍然不清, 基于浅层精细结构, 并结合断裂带两侧地层记录、精确年代学等资料, 有望对新生代以来研究区的构造变形历史提供更为有力的约束.

References

- Cowgill E, Yin A, Feng W X, et al. 2000. Is the North Alayn fault part of a strike-slip duplex along the Alayn Tagh fault system?[J]. *Geology*, 28(3): 255-258.
- Cowgill E, Yin A, Harrison T M, et al. 2003. Reconstruction of the Alayn Tagh fault based on U-Pb geochronology: Role of back thrusts, mantle sutures, and heterogeneous crustal strength in forming the Tibetan Plateau[J]. *Journal of Geophysical Research: Solid Earth*, 108(B7): 2346.
- Deng Y, Levandowski W, Kusky T. 2017. Lithospheric density structure beneath the Tarim basin and surroundings, northwestern China, from the joint inversion of gravity and topography[J]. *Earth*

- and *Planetary Science Letters*, 460: 244-254.
- Gao R, Li P, Li Q, et al. 2001. Deep process of the collision and deformation on the northern margin of the Tibetan Plateau: Revelation from investigation of the deep seismic profiles[J]. *Science in China Series D: Earth Sciences*, 44: 71-78.
- Gao S, Cowgill E, Wu L, et al. 2022. From left slip to transpression: Cenozoic tectonic evolution of the North Altyn Fault, NW margin of the Tibetan Plateau[J]. *Tectonics*, 41(3): e2021TC006962.
- Molnar P, Burchfiel B C, Liang K, et al. 1987. Geomorphic evidence for active faulting in the Altyn Tagh and northern Tibet and qualitative estimates of its contribution to the convergence of India and Eurasia[J]. *Geology*, 15(3): 249-253.
- Molnar P, Dayem K E. 2010. Major intracontinental strike-slip faults and contrasts in lithospheric strength[J]. *Geosphere*, 6(4): 444-467.
- Shi D N, Yu Q F, Poupinet G, et al. 2007. Crustal structures across the Altyn Tagh fault imaged by teleseismic receiver functions and their geodynamic implications[J]. *Acta Geologica Sinica*, 81(1): 139-144 (in Chinese).
- Wang D, Zhao B, Yu J, et al. 2020. Active tectonic deformation around the Tarim Basin inferred from dense GPS measurements[J]. *Geodesy and Geodynamics*, 11(6): 418-425.
- Wittlinger G, Tapponnier P, Poupinet G, et al. 1998. Tomographic evidence for localized lithospheric shear along the Altyn Tagh fault[J]. *Science*, 282(5386): 74-76.
- Wu C, Xu T, Tian X, et al. 2024. Underthrusting of Tarim lower crust beneath the Tibetan Plateau revealed by receiver function imaging[J]. *Geophysical Research Letters*, 51: e2024GL108220.
- Xu X, Zuza A V, Yin A, et al. 2021. Permian plume-strengthened Tarim lithosphere controls the Cenozoic deformation pattern of the Himalayan-Tibetan orogen[J]. *Geology*, 49(1): 96-100.
- Yin A, Harrison T M. 2000. Geologic evolution of the Himalayan-Tibetan orogen[J]. *Annual Review of Earth and Planetary Sciences*, 28(1): 211-280.
- Yin A, Rumelhart P, Butler R, et al. 2002. Tectonic history of the Altyn Tagh fault system in northern Tibet inferred from Cenozoic sedimentation[J]. *Geological Society of America Bulletin*, 114(10): 1257-1295.
- Yue Y, Liou J G. 1999. Two-stage evolution model for the Altyn Tagh fault, China[J]. *Geology*, 27(3): 227-230.
- Yue Y, Ritts B D, Graham S A, et al. 2004. Slowing extrusion tectonics: Lowered estimate of post-Early Miocene slip rate for the Altyn Tagh fault[J]. *Earth and Planetary Science Letters*, 217(1-2): 111-122.
- Zhang L, Unsworth M, Jin S, et al. 2015. Structure of the Central Altyn Tagh Fault revealed by magnetotelluric data: New insights into the structure of the northern margin of the India-Asia collision[J]. *Earth and Planetary Science Letters*, 415: 67-79.
- Zhao J, Mooney W D, Zhang X, et al. 2006. Crustal structure across the Altyn Tagh Range at the northern margin of the Tibetan Plateau and tectonic implications[J]. *Earth and Planetary Science Letters*, 241(3-4): 804-814.

附中文参考文献

- 史大年, 余钦范, Poupinet G, 等. 2007. 阿尔金断裂带附近地壳结构的接收函数成像及其地球动力学意义[J]. *地质学报*, 81(1): 139-144.